



Tree Physiology 00, 1–14
doi:10.1093/treephys/tpt002

Research paper

Modulation of bud survival in *Populus nigra* sprouts in response to water stress-induced embolism

Tête Séverien Barigah^{1,2*†}, Marc Bonhomme^{1,2†}, David Lopez^{1,2}, Amidou Traore³, Marie Douris^{1,2}, Jean-Stéphane Venisse^{1,2}, Hervé Cochard^{1,2} and Eric Badel^{1,2†}

¹INRA, UMR547 PIAF, F-63100 Clermont-Ferrand, France; ²Clermont Université, Université Blaise-Pascal, UMR547 PIAF, BP 10448, F-63000 Clermont-Ferrand, France;

³INRA, UR 0370 QuaPA, F-63122 Saint-Genès-Champanelle, France; *Corresponding author (tete.barigah@clermont.inra.fr)

Received May 30, 2012; accepted January 13, 2013; handling Editor Menachem Moshelion

Understanding drought tolerance mechanisms requires knowledge about the induced weakness that leads to tree death. Bud survival is vital to sustain tree growth across seasons. We hypothesized that the hydraulic connection of the bud to stem xylem structures was critical for its survival. During an artificial drastic water stress, we carried out a census of bud metabolic activity of young *Populus nigra* L. trees by microcalorimetry. We monitored transcript expression of aquaporins (AQPs; plasma membrane intrinsic proteins (PIPs), X intrinsic proteins (XIPs) and tonoplast membrane intrinsic proteins (TIPs)) and measured local water status within the bud and tissues in the bearer shoot node by nuclear magnetic resonance (NMR) imaging. We found that the bud respiration rate was closely correlated with its water content and decreased concomitantly in buds and their surrounding bearer tissues. At the molecular level, we observed a modulation of AQP pattern expressions (PIP, TIP and XIP subfamilies) linked to water movements in living cells. However, AQP functions remain to be investigated. Both the bud and tree died beyond a threshold water content and respiration rate. Nuclear magnetic resonance images provided relevant local information about the various water reservoirs of the stem, their dynamics and their interconnections. Comparison of pith, xylem and cambium tissues revealed that the hydraulic connection between the bud and saturated parenchyma cells around the pith allowed bud desiccation to be delayed. At the tree death date, NMR images showed that the cambium tissues remained largely hydrated. Overall, the respiration rate (R_{CO_2}) and a few AQP isoforms were found to be two suitable, complementary criteria to assess the bud metabolic activity and the ability to survive a severe drought spell. Bud moisture content could be a key factor in determining the capacity of poplar to recover from water stress.

Keywords: aquaporins, cavitation, 3D imaging, hydraulic, metabolic activity, NMR, respiration, water content, tree.

Introduction

Global climate changes are expected to exacerbate the negative effects of water deficiency by increasing the temperatures worldwide and changing the rainfall patterns (IPCC 2007). Among the predicted effects, the increasing frequency and intensity of extreme climatic events such as drought are expected to impact trees and forests. Drought stress leads to

numerous physiological effects on several traits related to water transport in trees, such as stomatal behaviour (Sperry et al. 1998, Hacke 2000, Domec et al. 2006), photosynthetic capacity (Brodribb and Feild 2000), turgor loss point of leaf cells (Alder et al. 1996, Brodribb et al. 2003) and water transport efficiency of the xylem (Tyree and Zimmermann 2002, Holbrook and Zwieniecki 2005). Because of the tensions

[†]These authors contributed equally to the work.

under which it operates, the xylem is potentially sensitive to water deficit and the danger of cavitation (Grace 1993). Xylem cavitation is a physical phenomenon that leads to embolism of the hydraulic system. Xylem conduits become air-filled and lose their functionality (Sperry et al. 1996, Tyree and Zimmermann 2002). As a direct consequence, the hydraulic system can no longer supply water properly to leaves and other tissues, including the meristematic zones. Within these zones, aquaporins (AQPs) may play a major role in cell membrane regulation of water permeability (Kaldenhoff et al. 2008).

Temperate trees develop terminal and axillary buds during the summer to protect the meristematic zone and leaf primordia against unfavourable winter conditions and allow the production of new shoots in spring. The success of new organ development depends on the firm establishment of efficient pathways for the supply of carbon, water and mineral nutrients that are delivered to the growing tissues through the phloem and xylem (Wardlaw 1990). The production of such structures is controlled by growth regulators (Ye 2002). Consequently, any adverse factor that impairs bud vitality may be life-threatening for the tree.

Bud break quality is strongly dependent on the previous year's environmental conditions (Herter et al. 1988, Escobedo and Crabbe 1989, Egea and Burgos 1994, Cook and Jacobs 2000). Thus drought stress, which affects the development of buds, may impact their survival capacity (Marks 1975, Lavender 1991). Brodribb and Cochard (2009) demonstrated the major roles that stem and leaf hydraulics play in determining the drought tolerance of conifers, but did not consider the fate of buds during and after water deprivation. Bud connections with the xylem network have rarely been addressed in trees, and hydraulic conductance data at the base of buds are limited. A recent study on *Fagus sylvatica* L. showed a positive correlation between the number of leaf primordia in the bud before budburst and the hydraulic conductance of the xylem vascular system connected to this bud (Cochard et al. 2005) without establishing the nature of the bud water feeding pathway. We still lack detailed information on how the buds are supplied with minerals and water from the bearer stem and on the impact of drought on bud survival.

Although buds are fed through connections with the stem, they are generally considered to be relatively independent appendages because their vascular connections to the xylem are non-functional until near bud break (Aloni 1987, Bartolini and Giorelli 1994), and because the symplasmic pathway is blocked during winter (van der Schoot and Rinne 1999). The recent review on vascular development by Ye (2002) introduced molecular approaches in plant models. Works on *Arabidopsis* improved knowledge of the dynamics of this development and the location of connections (Berleth et al. 2000, Grbic and Bleecker 2000, Kang et al. 2003), the role of auxin produced by leaf primordia in the bud (Bennett et al. 2006),

the role of auxin sink strength of the stem (Ongaro et al. 2008) and the role of cytokinin (Aloni et al. 2005). However, there are a few specific studies on the buds of trees. In particular, the mechanisms of water storage and water transport that may be involved in their drought resistance through apoplastic and cell-to-cell pathways are poorly documented (Rinne et al. 1994, Bréda et al. 2006).

At the cellular level, AQPs play a central physiological role in the regulation of the plant–water relations because of their biological membrane location and their functional involvement in the water transport across these membranes (Kaldenhoff et al. 2008). The AQPs belong to the ubiquitous superfamily of major intrinsic proteins (MIP) (Maurel et al. 2008). In plants, they typically fall into four main homologous subfamilies, of which plasma membrane intrinsic proteins (PIPs) and tonoplast membrane intrinsic proteins (TIPs) are the most abundant in the plasma and tonoplast membranes, respectively. Recently, a fifth uncategorized subfamily, designated X intrinsic proteins (XIP), was characterized in some plant species (Danielson and Johanson 2008). *Populus* encompasses this subfamily, with nine members. Knowledge of the XIPs remains partial; some XIP members are located in the plasma membrane and show water transport capacity (Danielson and Johanson 2008, Bienert et al. 2011, Lopez et al. 2012). Because biological membranes are potential barriers to passive transcellular water flow, PIPs and TIPs (and possibly XIPs) can control a large part of the cell water permeability and tissue hydraulic conductivity (Kaldenhoff et al. 2008). Their activity is finely regulated at the transcriptional and translational levels (Maurel et al. 2009), particularly in response to environmental factors, such as water deficit (Maherali et al. 2004, Alexandersson et al. 2005, Lopez et al. 2012). The steady-state level of AQP transcripts offers a suitable marker for monitoring any tissue–water relations involved in the cell-to-cell pathway. However, the functional roles of AQPs in water transport toward the buds are still poorly documented.

Here, we hypothesized that bud behaviour was a key factor for tree survival during a drastic water stress. We investigated the behaviour of the buds during a drastic water stress of poplars for several weeks. We hypothesized that the rapid xylem embolism would break the hydraulic connections to the buds and that this process would lead to the interruption of the water and nutrient supply to the buds. These buds would rapidly become isolated, dry and die, preventing the tree from sprouting again. Assuming that a bud respiration decrease would be one of the first indicators predicting plant death, we investigated whether this loss of vitality might be related to the lack of availability of water for the bud. Thus we monitored the axillary bud metabolic activity by measuring respiration rate by microcalorimetry. We investigated the local water distribution and status in buds and other surrounding bearer tissues using nuclear magnetic resonance (NMR) imaging. Moreover, we assessed

the responses of buds and their surrounding tissues in terms of water permeability by studying the expression and modulation of PIP, XIP and TIP AQP transcripts using quantitative real-time polymerase chain reaction (qPCR).

Materials and methods

Plant material, growth conditions and experimental design

We chose poplar (*Populus nigra* L.) as a model tree because of its fast growth rate and pronounced responses to environmental conditions, notably drought and other abiotic factors, and its worldwide research status (Bradshaw et al. 2000). We planted a single cutting of *P. nigra* per pot in a total of 64 black plastic 20-l pots in a glasshouse at Blaise-Pascal University (Clermont-Ferrand, France) on 13 November 2009. We filled the pots with a 2 : 1 v/v mixture of homogenized clay loamy soil and peat. We watered the plants to field water capacity every day for 3 months with tap water using a timer-controlled drip irrigation. We then split the trees into eight groups of six individuals each plus a single set of 16 control plants. From February to April 2010 we stopped watering the plants in the eight groups selected for the treatment to induce a drastic water stress, and we continued to water the control plants every day as before to field water capacity throughout the experiment.

Every 30 min we recorded night and day air temperatures (20 °C/22 °C) and relative humidity in the glasshouse. Night-time air relative humidity was high (up to 94%) but it could decrease to 55% when lights came on at ~4 a.m. Diurnal photosynthetically active radiation (PAR) in the glasshouse was ~1000 $\mu\text{mol m}^{-2} \text{s}^{-1}$ over the waveband 400–700 nm and was provided by 400 W Master son-T Pia Hg Free lamps (Philips Lighting France, Suresnes, FRA). The photoperiod was 8/16 h night and day. We measured PAR every 5 s (an Li-190SA quantum sensor, Li-Cor Inc., Lincoln, NE, USA), and stored 10 min average values in a 21X data logger (Campbell Scientific, Shepshed, UK).

Experimental protocol during water stress

During the period of water deprivation, we conducted eight samplings 0, 14, 18, 21, 25, 28, 32 and 61 days after the start of treatment. At each date, we focused on a set of six water-stressed plants and two control plants. We measured the predawn leaf water potential and then harvested the sprouts from the sampled trees. We cut the stem at 50 mm above the soil and divided it into four parts. From the proximal to the distal end, we used a first 20-mm-long segment, which bore one bud, for NMR observations, a second 20-mm-long segment, which bore also one bud, for molecular analyses, a third segment with 10–15 buds, which was 200 mm long, for heat flow and respiration rate measurements, and a last 50-mm-long segment to evaluate the percent conductivity loss. Finally, we

re-watered the stumps of the sampled trees to field capacity every day. Four weeks after the sampling date we evaluated the total tree survival rate as the number of stumps from stressed trees that were still able to re-sprout.

Predawn water potential measurements

We measured predawn leaf water potential for fully exposed healthy undamaged leaves borne on sprouts. We used a Scholander-type pressure chamber (PMS, Corvallis, OR, USA) to assess plant water status (Scholander et al. 1965, Hinchley et al. 1992). We collected two bagged leaves per stressed and control tree to determine their predawn leaf water potential (Ψ_p). We wrapped these leaves in an aluminium foil and sealed them in a plastic bag the evening before sampling to prevent transpiration and promote water tension equilibrium between the sprout axis and root zone overnight. At the sampling time we removed the bagged leaf from the sprout and promptly placed it in the pressure chamber without removing the plastic bag (Turner 1988, Ameglio et al. 1999). We completed Ψ_p measurements every sampling date until the plants had shed almost all their leaves in 3–4 weeks.

Nuclear magnetic resonance imaging

We wrapped both end-cuts of each sampled stem segment in Parafilm®, placed them in a sealed NMR tube to prevent sample water loss, and took them immediately to the NMR facility (INRA, Clermont-Ferrand/Theix, France). We performed proton magnetic resonance imaging (MRI) experiments at 400 MHz in a 9.4 T vertical wide-bore (89 mm diameter) spectrometer equipped with Micro2.5® micro-imaging accessories (Bruker Biospin, Ettlingen, Germany). We used a 15 mm ^1H -imaging birdcage coil in the imaging probe for the radio frequency (RF) transmission and signal reception. To reduce transpiration during the imaging process, we wrapped the sample a few centimetres beyond its proximal end with a plastic film. We then inserted the bud in the 13 mm diameter NMR tube. For calibration purposes we inserted a 0.5 mm glass capillary filled with 500 $\mu\text{mol l}^{-1}$ MnCl_2 -doped water (allowing a water proton T2 relaxation time of 40 ms at 400 MHz) into the NMR tube close to the sample. We centred each sprout in the RF coil using foam supports. We performed all the experiments at room temperature (~21 °C).

We applied two kinds of imaging sequence to map the local water distribution in different tissues and collect information about the degree of binding of water. We acquired T2-weighted images using a multi-spin multi-echo (MSME) pulse sequence on a volume of 10 contiguous slices, 0.75 mm thick, centred on the bud location to generate the map of the T2 relaxation times (T2 parametric map). For each slice, we recorded six echo times (TE) ranging from 11 to 66 ms; 11 ms with the following parameters: time to repetition (TR) 2000 ms, field of view (FOV) 10 mm and matrix size 256 × 256 allowing an in-plane resolution of 39 μm^2 . We performed these acquisitions on both

transverse and longitudinal planes for a total acquisition time of 13 min.

For structure analysis, we selected a region of interest of $10 \times 10 \times 10$ mm for 3D anatomical imaging that covered the bud and its surroundings. We used a 3D proton density rapid acquisition with relaxation time enhancement pulse sequence with the following parameters: TR/TE 1300/9 ms, acceleration factor (AF) 4. The final volume image was $256 \times 256 \times 256$ voxels with a resulting isotropic voxel resolution of $39 \mu\text{m}^3$. We performed two scans per sample and averaged the data.

We carried out NMR measurements on two individuals per sampling date: 0, 21, 28, 32 and 61 days after water stress onset (total 10 individuals). We computed the parametric images (proton density and T2 maps) by fitting the decay of the signal intensity (S) with echo time (TE) to $\ln(S) = -TE/T2$ using linear regression. The local proton density (signal intensity extrapolated for TE = 0 ms) and the T2 maps were then processed by image analysis using ImageJ software (Rasband 1997–2009) on radial-tangential cross sections and on radial-longitudinal sections. We calibrated the proton density images using the glass capillary content as a reference. Diametrical $540 \mu\text{m}$ (15 pixels) thick profiles were then plotted in the middle plane, which included the centre of the bud. We used these profiles to extract the variations in bark, xylem, cambium (which includes here the living cells of xylem), pith (for convenience, we use the term 'pith' for the central part, which comprises the pith and its surrounding parenchyma cells) and bud proton densities. Finally, we extracted the maximum and mean values of proton density. In the same way, we extracted the maximum and mean of the characteristic relaxation time of water from the T2 parametric image. For these T2 measurements, we focused on exactly the same regions of interest as for proton images.

Native state embolism measurements

Native state embolism refers to the percent loss of conductivity (PLC) that occurs as a consequence of the water stress experienced by an intact plant in situ. We measured the native state percent embolism with a xylem embolism meter (XYLEM, Bronkhorst, Montigny-les-Cormeilles, France; http://www.bronkhorst.fr/files/br_fr/xylem2.pdf) on the specimens and control plants. We collected the sprouts in the morning, put them in wet black plastic bags and brought them immediately to the laboratory for hydraulic conductance measurements. We cut the 5 cm stem segments under water from the sprouts and fitted them to water-filled tubing. We connected one end to a tank of a de-gassed, filtered ($0.2 \mu\text{m}$) solution containing $100 \text{ mmol KCl l}^{-1}$ and $10 \text{ mmol CaCl}_2 \text{ l}^{-1}$. We recorded the flux of this solution through a stem segment section under low pressure (6 kPa) as initial hydraulic conductance (k_{ini}). We then perfused the stem segments at least twice with the same filtered solution at 0.2 MPa for 2 min to remove air from embolized vessels and determined maximum hydraulic conductance

(k_{max}). Percent loss of conductivity (PLC) was determined for each stem segment as $\text{PLC} = 100 \times (1 - k_{\text{ini}}/k_{\text{max}})$ (1).

Bud metabolic heat rate and respiration rate measurements

Plant calorimetry offers an approach for assessing the metabolic activity of living tissues (Hansen et al. 1997, 2004, Llamas et al. 2000). We used this approach to carry out a census of dry-down impacts on bud ability to burst in re-watering stressed plants. For each sampling date, we measured the metabolic heat rate (Rq) and respiration rate (Rco_2) of buds at 20°C . We collected 10–15 buds depending on their size, as a minimum of fresh matter is required to run the micro-calorimeter. We measured their fresh weight and inserted them into a 1 cm^3 micro-calorimeter cell. The measurements were made with differential scanning calorimeters (micro DSC VII, SETARAM, Caluire, France). Micro-calorimetric procedures are described in Criddle et al. (1991). Briefly, the operating method involved three steps. Firstly, a heat flow was generated in the cell (continuously recorded) until a steady state (q_1) was reached in roughly 20 min. Secondly, we inserted a small capsule with $20 \mu\text{l}$ of 1 N NaOH into the measurement cell. The NaOH reacts with the CO_2 released by the respiration of the tissues. This reaction resulted in an additional heat flow, which led to a new steady state (q_2). Thirdly, we removed the capsule and the heat flow decreased to a new steady state (q_3 ; equal or close to q_1 if no alteration of the living system occurred during the measurement process). Lastly, we estimated the metabolic heat flow as the mean values of q_1 and q_3 , and the respiration flow as the difference between q_2 and the metabolic heat flow value.

We retrieved, dried at 70°C for 24 h and weighed the samples to determine their dry masses (Dw). Finally, we calculated the metabolic heat rate and respiration rate according to Hansen et al. (1989) and Hansen and Criddle (1990). The metabolic heat rate corresponding to the metabolic heat flow per unit dry mass (Eq. (2)) was expressed in $\mu\text{W mg}^{-1}$, and the respiration rate as the flow of CO_2 per second and per dry mass unit and expressed in $\text{nmol CO}_2 \text{ g}^{-1} \text{ s}^{-1}$ (Eq. (3)):

$$\text{Rq} = (q_1 + q_3) / (2\text{Dw}) \quad (2)$$

$$\text{Rco}_2 = (q_2 / \text{Dw} - \text{Rq}) / 108.5 \quad (3)$$

We carried out five replicates at each sampling date and we recorded the mean values. We also measured the bud moisture content as weight of water divided by dry mass.

Total RNA isolation, cDNA synthesis and amplification

We performed molecular investigations at Day 28. We extracted the total RNA from buds, bark (including phloem and cambium tissues) and wood (i.e., xylem without cambium) at the

intermediate part of the stem using CTAB extraction buffer according to Chang et al. (1993). First-strand cDNA was synthesized from 1 µg of total RNA using SuperScript III (Invitrogen, Carlsbad, CA, USA) following the manufacturer's instructions. We performed the real-time PCR amplification using a MyiQ thermocycler (Bio-Rad, Hercules, CA, USA) with MESA GREEN qPCR MasterMix Plus (Eurogentec, Seraing, Belgium) containing 2 µl of 40-fold diluted cDNA according to the manufacturer's protocol. The thermal profile of the reaction was: 94 °C for 3 min, 40 cycles (94 °C for 20 s, 54 °C to 58 °C for 20 s and 72 °C for 20 s). We verified the specificity of amplicons by melting curve analysis, and checked them by gel electrophoresis. We deduced PCR efficiencies for each gene from series of diluted cDNA (Pfaffl 2001). The crossing cycle number (C_t) was automatically determined for each reaction by the iCycler iQ v2.0 software with default parameters. Normalization of the target gene abundance was achieved using the geometric mean of three reference genes (*18S rRNA*, *EF1α*, *SAND* for a final geometric mean of $C_t \pm$ standard deviation = 18.02 ± 0.83). We chose these candidates from different protein families to reduce the possibility of co-regulation. We assessed the MIP transcript steady-state levels in each vegetative tissue by comparison of their mean of C_t after normalization with the geometric mean of the reference gene C_t . Expression levels were graphically represented after distribution and scoring on an arbitrary range between 0 and 100. A C_t of 20 was assigned an arbitrary value of 100 (corresponding to the highest MIP expression level in our condition, here *PIP1;2*); a C_t of 40 was given an arbitrary value of 0 (no expressed gene). We then assigned all the other C_t values between 0 and 100, scaled based on their relative distributions. For the evaluation of the differential expression of MIP transcript in response to stresses in each tissue, we computed the relative changes using the equation $\log_2(2^{-\Delta\Delta C_t})$ equation according to the procedure of Pfaffl (2001). The mean C_t value was determined from two independent biological replicates for each sample, and every PCR reaction was carried out in triplicate. All the primers used for this study were designed with Primer3plus application (<http://www.bioinformatics.nl/primer3plus>) (Rozen and Skaletsky 2000) and are listed in the Supplemental Data available at *Tree Physiology* Online (Table S1).

Data analysis

Aquaporin steady-state levels for each biological assay were computed by one-way analysis of variance (ANOVA) followed by a Tukey's honestly significant difference (HSD) post hoc test ($P < 0.05$). Data of heat flows and respiration rates are given as mean \pm standard error (SE). The comparisons of predawn water potential of the plants, bud heat flows and respiration rates over time were computed with the repeated data collected on each sampling date using the non-parametric test of Kruskal–Wallis. We computed ANOVA and the

non-parametric tests using the R software package (R Development Core Team 2011; R Foundation, <http://www.r-project.org/>) and made non-linear curve fittings using the SigmaPlot 9.0.1 software package (SigmaPlot, Systat Software Inc., Point Richmond, CA, USA; Systat Software, <http://www.systat.com/>).

Results

Variation in predawn leaf water potential, PLC, bud respiration rate, proton density and bud moisture content during water stress

The predawn leaf water potential Ψ_p decreased significantly ($P = 0.003$) within the first 14 days after the onset of water deprivation (Figure 1a). In a second phase, Ψ_p kept a stable value for 7 days. Meanwhile, the stem segments lost their water transport ability. The plants shed almost all their leaves within 2 days, 3 weeks after water stress inception. Consequently, no further measurement of the predawn leaf water potential was possible. Stem segment PLC increased with time in a sigmoid pattern from the start of the water stress treatment (Figure 1b). The loss of conductivity reached 50% after 16 days of water stress and 90% after 4 weeks of water deprivation. Bud metabolic heat and respiration rates showed similar patterns (Figure 1c). They decreased significantly ($P = 0.009$) during the first 18 days, respectively, from 29.1 ± 2.8 (SE) to 11.8 ± 0.5 nmol CO₂ g⁻¹ s⁻¹ for bud respiration and from 7.7 ± 0.4 to 4.9 ± 0.1 µW mg⁻¹ for metabolic heat rate. This weak respiration rate remained at a steady state ($P = 0.46$) for at least 14 days before decreasing to 1.8 ± 1.5 nmol CO₂ g⁻¹ s⁻¹. Measurements on NMR images showed that the proton density could reliably discriminate among the different components of the stem segment at the bud level (Figures 1d and 2). Proton density was higher in bud tissues than in pith, cambium, xylem and bark. For all the tissues studied, a decrease in proton densities occurred over time: the decrease was very low for both the bark and the xylem, but was marked for the bud, pith and cambium. The bud moisture content ranged from 0.4 ± 0.3 to 2.1 ± 0.1 . However, the moisture content of most of the buds was close to 1.3. We found a close relationship between bud moisture contents and respiration rates (Figure 3a) and also between proton density values (Figure 3b). After watering for 4 weeks, all the stumps recovered from their dry-down episode (data not shown). Only the trees that had experienced 61 days of water stress died.

Local water availability and its distribution in bud and shoot bearers

Three weeks after the inception of the water stress treatment, the xylem tissues were largely embolized (Figure 2), while all the other stem tissues remained consistently hydrated. In the next steps, proton imaging showed that the bud remained

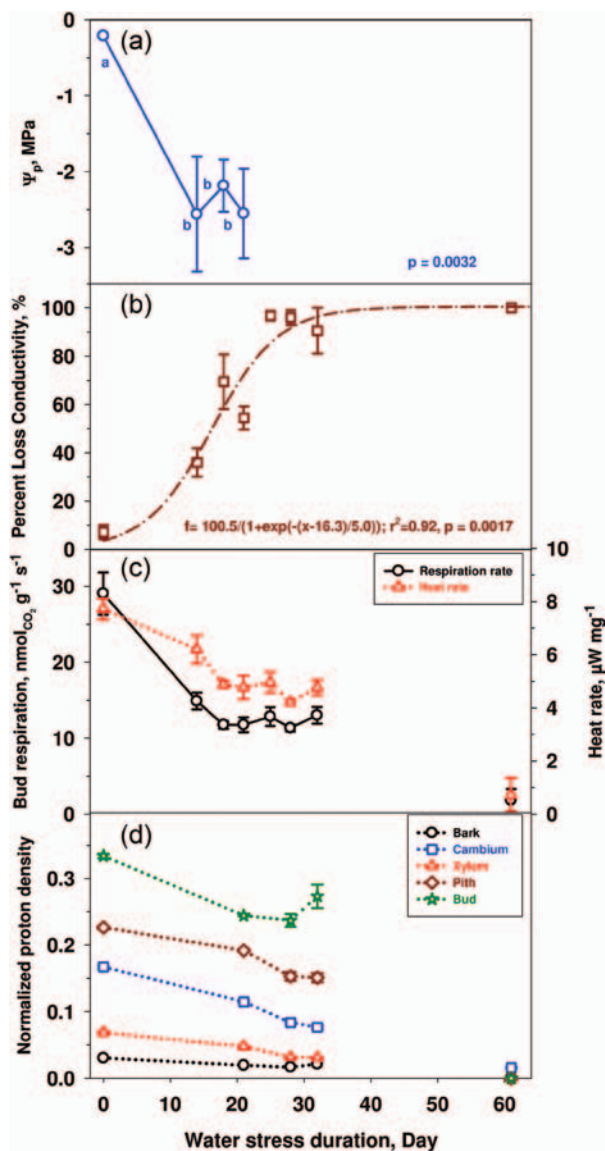


Figure 1. Patterns of predawn leaf water potential (a), percent loss of conductivity of the stem (b), bud heat rate and respiration rate (c) and normalized proton density (d) over the sampling periods of time. Symbols represent means and error bars are standard errors (SE) of the means ($n = 5$) at each sampling date. The alphabets are used to split the differences in water potential over time. Values with different letters are significantly different at the 0.05 level (Kruskal–Wallis' test). Leaf water potential was not available after the leaves had fallen. Values of control plants are merged in the 0 date.

highly hydrated despite the almost complete embolism of the xylem. The base of the bud seemed hydraulically connected to the cambial area, which showed the highest proton density. Similarly, the base of the bud was hydraulically connected to the pith (Figure 4, white arrowhead). This connection crossed the xylem, even when parts were fully embolized. The central part of the pith appeared water-free, but a layer of surrounding tissue was strongly hydrated (Figure 2, white arrow).

The maximum proton density was found in the peripheral zone of the stem where the living cells are located. This zone

includes the cambium area where the cell divisions occur. This area also showed the highest values for T2 (Table 1) at > 30 ms, indicating a low degree of binding of water, which was therefore easily movable and usable. The pith area was also highly hydrated. Nevertheless, it showed a lower T2 than cambium area (~ 20 ms). Thus although water was present, it seemed to be less movable and so less usable by surrounding tissues. Other tissues such as bud and xylem showed lower moisture content. Even though all the tissues of stressed plants remained highly hydrated compared with the control (Figure 1), their proton density clearly decreased during the first 3 weeks of the treatment. They then remained stable for at least 12 days. Finally, the proton density decreased to zero from Day 32 to Day 61. It reached zero in the bud and in the pith areas. However, water remained in the peripheral tissues of the stem, including the cambium and bark tissues, which were the last to keep water.

Whether we used the mean or the maximum value (data not shown), the patterns of proton density and T2 curves over time were similar. The high value of the relaxation time in the cambium area decreased steadily over time. The value of the T2 became very low (~ 10 ms), and three times lower than before the water stress treatment. The T2 value was initially lower for the bud than in the cambium area, but it remained fairly stable (~ 14 ms) until Day 32, i.e., for 4–5 weeks under water-stressed conditions. At the end of the experiment, the T2 value of bud decreased to a very low value of around 4 ms. This value needs careful analysis because the proton density was close to zero in this area. In the pith, the relaxation time remained stable (between 15 and 19 ms) until Day 32 and then decreased to zero on the last date. At this date, the proton density also became nil. In the bark, the time course was quite similar, showing a first stable plateau until Day 32 followed by a decrease to zero at the end of the experiment.

Expression pattern of AQP transcripts

The steady-state levels of transcript accumulation for the PIP, XIP and TIP subfamilies were simultaneously traced in the axillary buds and their immediate stem surroundings in wood (including xylem and pith) and bark (including phloem) from plants either well-watered or exposed to 28 days of the

Table 1. Relaxation time T2 obtained by NMR imaging using an MSME pulse sequence. Values are expressed in milliseconds and reflect locally the degree of binding of water in the tissues. Values of control plants are merged in the 0 column.

Elapsed time (days)	0	21	28	32	61
Pith (ms)	21.5 ± 0.9	18.3 ± 0.7	15.3 ± 0.7	17.5 ± 0.7	0.0 ± 0.0
Cambium (ms)	33.0 ± 0.9	31.0 ± 0.6	22.5 ± 0.9	19.5 ± 0.8	11.0 ± 1.0
Bud (ms)	18.5 ± 0.8	14.6 ± 0.8	13.5 ± 0.5	14.2 ± 0.6	4.1 ± 0.7

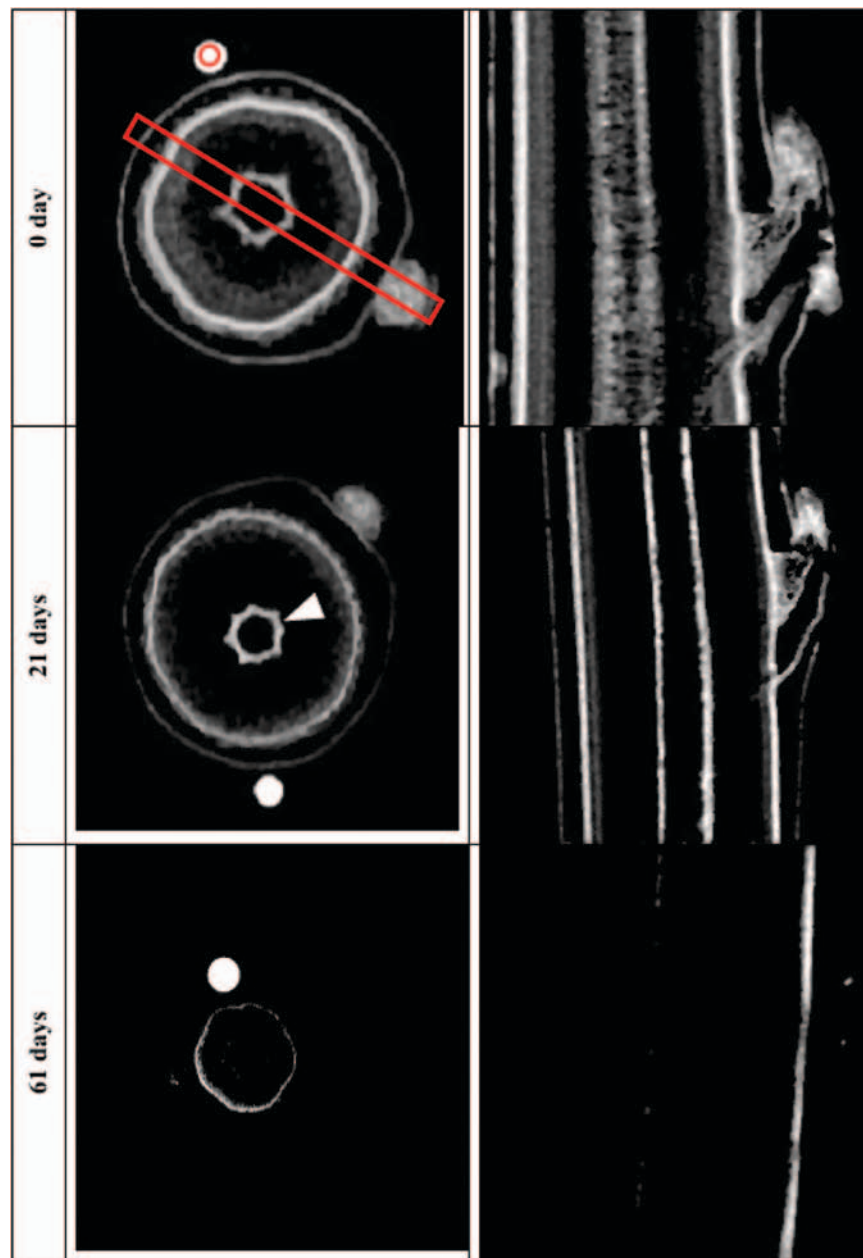


Figure 2. Three-dimensional MRI mapping of the shoot segments containing the bud. Grey levels are inversely proportional to the normalized proton density that reflects the water content. Bright discs show the capillary glass filled with doped water that allows the grey level calibration. The radial–tangential plane (left) and radial–longitudinal plane (right) were used for proton density measurements of tissues. The parenchyma tissues close to the pith and the cambium areas showed very high moisture contents. At the last step, the cambium remained hydrated, while the bud was already dry and dead. Spatial resolution is 39 μm .

described drastic water stress constraint (Figure 5). Of the 15 PIP, 9 XIP and 17 TIP members observed in the *Populus* genus (Lopez et al. 2012), all PIPs, 3 XIPs and 14 TIPs showed detectable expression in *P. nigra*. No XIP1s, XIP3;3, TIP1;2, TIP 5;1 and TIP5;2 transcripts were detected (data not shown). With the exception of XIP3;1 and XIP3;2, which were exclusively expressed in wood, all the other AQPs were ubiquitously expressed in buds, wood and bark in both control and stressed plants (data in boldface are significant and those not sharing

the same letters are significantly different; Tukey's HSD, $P < 0.05$, Figure 5). However, no clear organ specificity expression emerged, except for PIP2;5 and PIP2;8, which were preferentially expressed in wood and bud, respectively. Among the highly expressed AQPs (>50%), we observed all the PIP1s, 7 PIP2s (PIP2;1, PIP2;2, PIP2;3, PIP2;4, PIP2;6, PIP2;7, PIP2;10) and 7 TIPs (TIP1;3, TIP1;5, TIP1;6, TIP1;7, TIP2;1, TIP2;2, TIP4;1). Conversely, 4 AQPs (TIP1;1, TIP1;8, TIP3;1 and TIP3;2) were marginally accumulated (<25%). The XIP subfamily

showed the most sharply contrasted accumulations between organs where *XIP2;1* and *XIP3;2* were notably expressed in buds and wood, respectively, whereas *XIP3;1* remained marginally expressed.

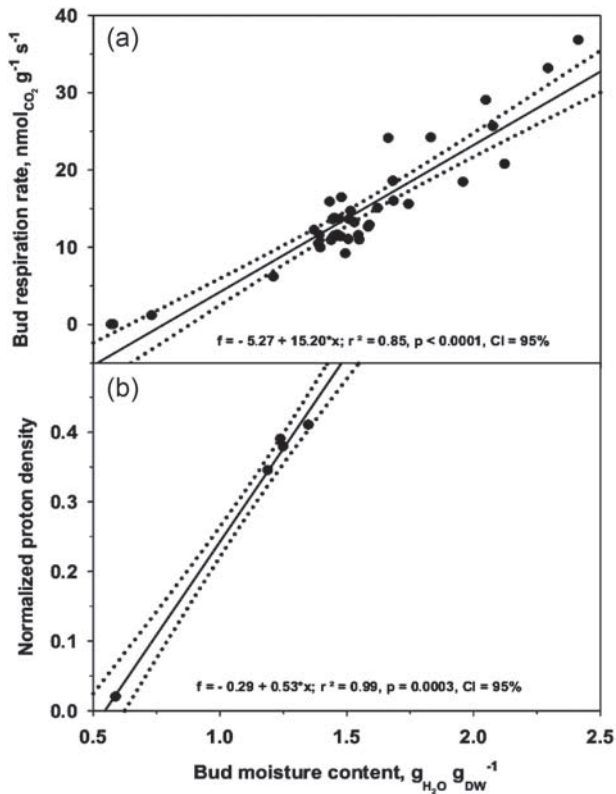


Figure 3. Relationship between bud moisture content, bud respiration rate (a) and normalized proton density (b) in *P. nigra*. Solid and dotted lines represent the regression line and confidence interval at 95%.

Among all the AQP members we monitored, only *PIP1;1* remained constant whatever the organs under water stress, whereas all the other members presented differential accumulation when plants were under water stress constraints. Overall, bark tissue presented the strongest response to water stress, with the significant modulation of 23 AQPs, among which 6 AQPs were upregulated (*PIP2;1*, *PIP2;9*, *TIP1;6*, *TIP2;3*, *TIP3;2*, *TIP3;1*) and 17 AQPs were downregulated. Wood tissue encompassed 13 modulated AQPs with two upregulations (*PIP1;3* and *TIP1;5*) and 11 downregulations, including the tissue-specific AQP, *XIP3;2*. For bud tissue, 15 AQPs were modulated: eight were upregulated and seven were downregulated. All were distributed over the three MIP subfamilies.

Discussion

Water stress impacts on plant water status and bud respiration rate

Severe water stress (8 weeks without watering) generated changes in some physiological processes for our juvenile poplar plants: predawn water potential, reduction in stem conductance or in respiration rate were observed and were typical responses for progressive stages of water stress (Figure 1a–c).

We found that our young poplar trees displayed an ability to keep their Ψ_p relatively constant for at least 2 weeks after a substantial drop, which occurred during the first 14 days after the inception of the water stress. This stabilization of Ψ_p may be under stomata control (Schulze 1993, Flexas et al. 2004, Thapa et al. 2011) or the ongoing leaf abscission (Munné-Bosch and Alegre 2004, Bréda et al. 2006). Our physiological observations are in line with those of Braatne et al. (1992), Hinkley et al. (1992) and Rood et al. (2000) who underlined

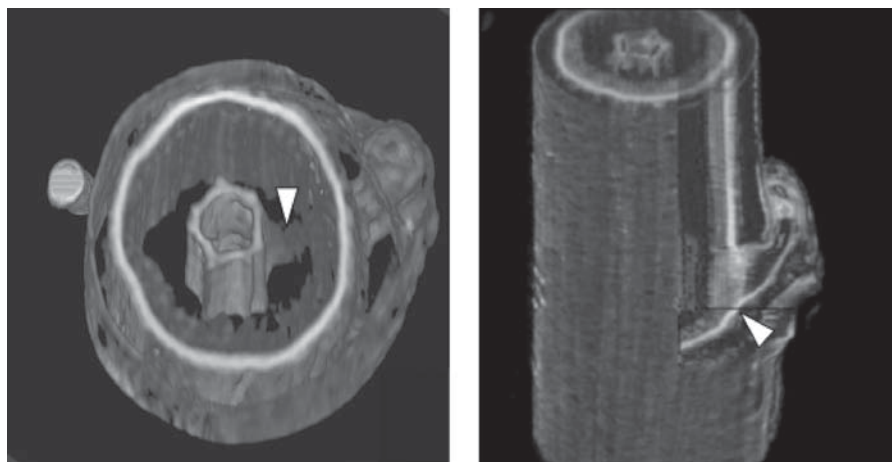


Figure 4. Three-dimensional visualization of the normalized proton density (MRI measurements) in the bud and the stem of poplar (*P. nigra*) during a water stress event (4 weeks). The proton density reflects the quantity of water contained in the tissues. These observations enlighten a large hydraulic connection between the bud and the parenchyma tissue (white arrowhead) that surrounds the pith (left) and the connection of the bud with the cambial area (right). The cambium was the most highly hydrated tissue, as the xylem area was almost fully embolized: the remaining water was concentrated around its peripheral zone, close to the cambium where living cells are located.

the substantial vulnerability of black poplars to prolonged drought. Our trees shed their leaves within 3 weeks after water stress inception. This could be due to the inability of the stomatal closure to maintain a favourable water balance, as leaf abscission is an effective, rapid reaction to temporary drought (Kozłowski and Pallardy 1997, Taiz and Zeiger 1998). In our case, leaf shedding seemed to delay fatal desiccation, as only plants deprived of water for >4 weeks failed to recover after re-watering.

The widespread embolism that occurred within the sprouts in a sigmoid-like pattern towards 100% water conductivity loss was expected (Tyree and Sperry 1988, Rood et al. 2000). Meanwhile, the total loss of conductivity seemed to coincide with total leaf shedding in the study plants (Figure 1a, b). This suggests a close relationship between embolism and leaf abscission and might be analysed as a physiological strategy of the plant to reduce the transpiration process. Reducing water loss may preserve the internal tissues, particularly the meristematic ones, from excessive desiccation (Blum 2009) and cessation of cellular metabolism.

According to de Fayé et al. (2000) and Monserrat-Martí et al. (2009), water stress alters bud formation, growth and burst. However, we did not observe any severe water stress effect on bud survival in this study, except for the trees that experienced >32 days of water shortage. Therefore, we suggest that there is a safety mechanism that allows the trees to slow down the lethal desiccation of their buds during a water shortage period by preserving part of their available water for vital living tissues including buds. The NMR images (Figure 2) provide new insights into a compartmentalization of the available water in the different tissues. They reveal that buds contained high free water density while xylem tissue became rapidly embolized during the water stress. Nuclear magnetic resonance images and conductivity measurement (PLC) were consistent with this finding (Figure 1b). The inner part of the xylem became rapidly non-conductive, while the peripheral zone still contained water for 4 weeks. In addition, the hydraulic connections of buds with highly hydrated tissues suggest possible mutual water exchanges. In particular, the bud seems to be hydraulically connected to the cambium area and to a ring of parenchyma cells located around the pith (Figures 2 and 4). Both areas are fully saturated with water. Also, the moisture content of the cambium and pith areas decreases in the same way as the bud. Again, this supports the hypothesis of functional hydraulic connections between those tissues even during a water stress event. The cambium area and the ring of parenchyma cells located around the pith remain hydrated at least as long as the buds. We therefore hypothesize that these structures may act as internal safety water reservoirs. Our observations are consistent with the diffusion-weighted images of poplar buds reported by Kalcsits et al. (2009). Cytological observations (Figure 6) show a large bundle of parenchyma cells that are

mainly oriented along the radial direction. This anatomical structure may allow an efficient radial transfer pathway of water between an inner reservoir and the bud. These results invalidate our initial hypothesis that the xylem embolism would lead to the rapid desiccation and death of the bud.

From Figure 1b and c, the embolism expansion pattern in the sprouts appears to be closely related to bud respiration rate limitation. We also found that bud respiration rate was closely correlated ($R^2 = 0.85$, $P < 0.0001$) with water content (Figure 3). Thus we suggest that the bud respiration rate and their water content are strongly coupled and not independent as previously reported by Huang et al. (1975), who underlined a rapid decline of respiration rate as a consequence of a developing water stress event. For Amthor (1994) and Gibon et al. (2009), the decrease in respiration rate was a result of reduced resource availability and substrate protein content. It has been reported that the metabolic heat rate and the respiration rate rely on tissue metabolic activity (Hansen et al. 1997, 2004, Llamas et al. 2000) and on bud growth capacity (Trejo-Martínez et al. 2009).

The steady-state pattern we observed for the respiration rate 2 weeks after the water stress inception could reflect the 'maintenance' cost of a basic bud metabolism. Thus we can reasonably hypothesize that any failure in sustaining the basic bud metabolism requirement will lead to vanishing bud metabolic heat and respiration rates and ensuing bud death. To our knowledge, there are no reported data in the literature on the bud maintenance respiration rate. Matheson et al. (2004) reported values ranging between 20 and 30 nmol CO₂ g⁻¹ s⁻¹ for shoots of *Verbascum thapsus* L., *Convolvulus arvensis* L., *Helianthus tuberosus* L. and *Avena sativa* L. seedlings. These values are closely correlated with the number of living cells in their samples. It is therefore likely that the low value we found in our experiment (12.2 nmol CO₂ g⁻¹ s⁻¹) for the bud maintenance respiration rate could result from the presence of the protective scales, which are composed of a tiny amount of living tissue. In addition, the associated metabolic heat rate (4.7 μW mg⁻¹) we record for poplar buds is close to that of dormant *Larix laricina* (Du Roi) K. Koch buds (Hansen et al. 1989) and *Vitis vinifera* L. buds (Gardea et al. 1994). Atkin and Macherel (2009) show how the dark respiration maintenance plays a major role in plant survival under water stress conditions and its rapid recovery of productivity after re-watering. Flexas et al. (2005) report that photosynthesis can stop completely in severe water shortage, while the respiration rate may either increase or decrease under stress, but never becomes totally impaired. Our results also show a close correlation between bud respiration rate and water content. Several mechanisms are probably involved in the maintenance of a minimum threshold level of bud moisture content to ensure a minimal activity and a maintenance respiration rate to keep the bud alive during increasing water stress duration. The survival of

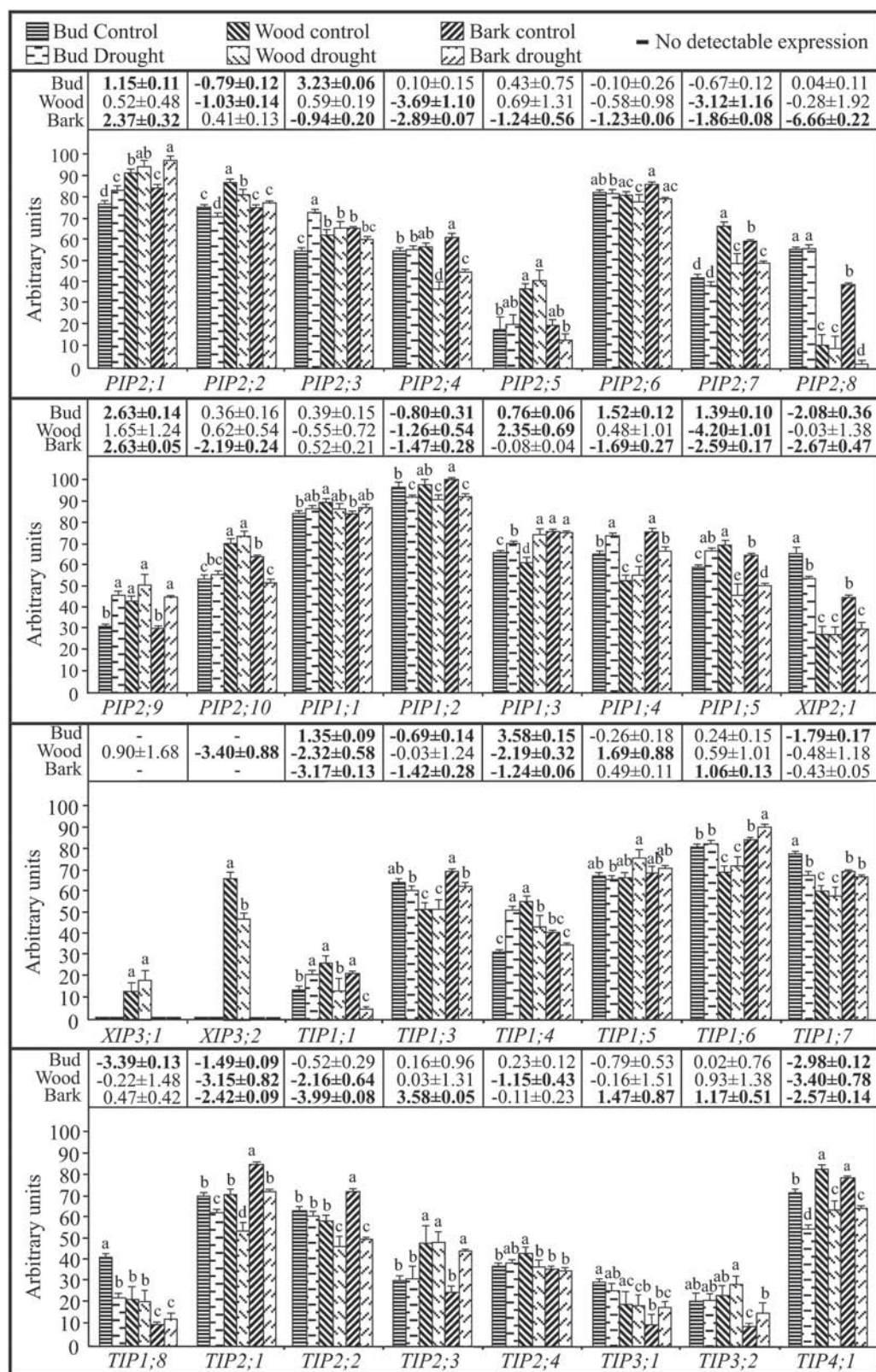


Figure 5. Expression patterns of *PIP*, *TIP* and *XIPs* isoforms in bud, wood and bark of *P. nigra* after 28 days of water stress exposure. Changes in expression levels for the three tissues are presented as expression ratio (water stressed vs. well-watered control). Steady-state level representation for each biological assay is given in the Materials and methods. Transcript expression levels were determined by real-time quantitative RT-PCR using specific primer sets for each isoform. The geometric mean of three reference genes was used as the endogenous control. Data correspond to the means of three technical replicates from two independent biological experiments, and bars represent standard error ($n = 2$). Three plants were pooled per biological sample. Data in boldface are significant and those not sharing the same letters are significantly different (Tukey's HSD, $P < 0.05$).

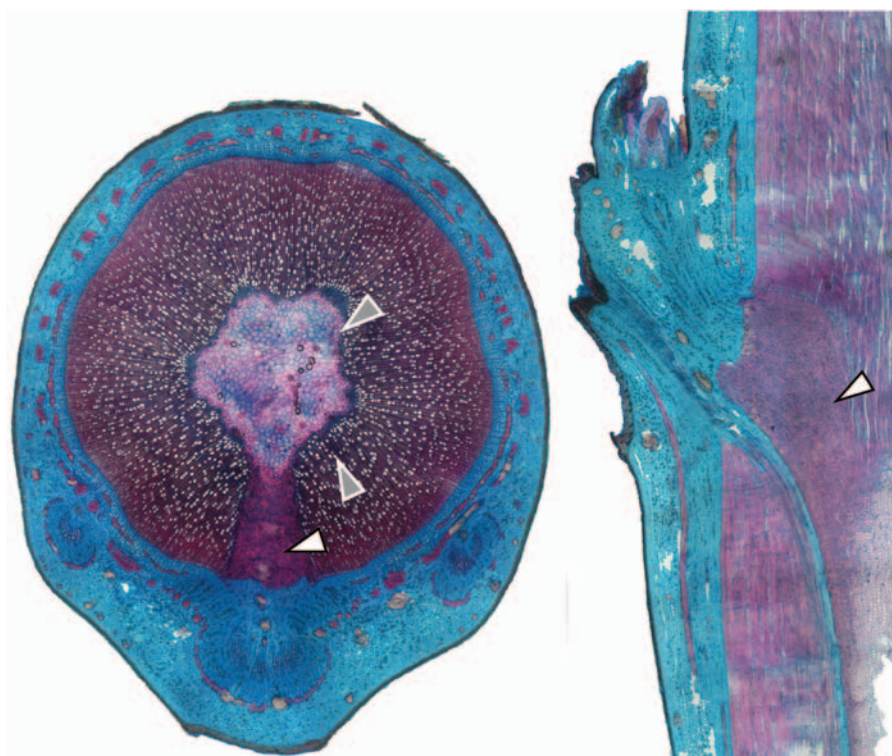


Figure 6. Cytological observations of the stem anatomy. Transverse slice (25 μm thick) shows the large connection between the bud and parenchyma tissue that surrounds the pith. The connection is made of a large bundle of parenchyma cells (white arrowhead) and allows a radial transfer of water between an inner reservoir (grey arrowhead) and the bud. The double staining method with safranin/astra blue was applied to microscopic sections. Red stain with Safranin is the indicator for lignin. Astra blue tints cellulose.

the meristematic cells is strongly dependent on the capacity to use carbohydrates to produce energy and the capacity to maintain minimally sufficient hydration in this structure (McDowell 2011). This capacity depends not only on the overall response of the plant through stomatal regulation, but also, at the tissue level, on the compartmentalization of the bud and the functional integrity of vascular connections between other tissues of the stem and the bud.

Aquaporin expression and water transport

Aquaporin expression patterns can be linked to our physiological and NMR imaging data. Stem xylem was the first embolized and showed the lowest reactive molecular responses. Hence living cells within the xylem seem unable to preserve their hydraulic reservoir. Conversely bark, and to a lesser extent buds, show the most marked molecular response together with the greatest number and magnitude of modulated AQP isoforms. This is consistent with the hypothesis that bark (as a reservoir) and bud (as a vital organ) both need to react to maintain their moisture content.

The *Populus* genus encodes 15 PIP, 9 XIP and 17 TIP members (Lopez et al. 2012). Although these isoforms are numerous, most of them are constitutively expressed and modulated in our experiment (Figure 5). It would nevertheless be unsafe to make any functional interpretations of each isoform pattern

in the different biological assays. However, an overall reading of PIP2s and PIP1s may offer us some physiological insight. PIP1s and PIP2s were predominantly upregulated or slightly modulated in buds, whereas both were essentially downregulated in the bark. This might reflect their ability to draw water upward and hold water. We still know very little about the physiological function of PIPs in woody plants: PIP1 isoforms are thought to have weaker water channel activities than PIP2 isoforms, but PIP1s probably play a substantial role in controlling water permeability, since coexpression of PIP1 with PIP2 isoforms potentiates water transport (Fetter et al. 2004, Secchi and Zwieniecki 2010). However, little information is available about the functions of TIP subfamily members which are known to attenuate plant susceptibility to water stress (Wang et al. 2011). Our results show that most modulated TIPs are downregulated during water stress, although some isoforms are upregulated, but in tissue-specific ways. Tonoplast membrane intrinsic proteins also provide osmotic potential balance for the cytoplasm by exchanging water with the vacuole. Thus the apparently conflicting patterns we observed could be explained by the different locations in which the isoforms are expressed. However, further investigation is still needed to clarify AQP involvement in these physiological processes. This investigation could be done using mutants or transgenic resources in which the expression of

specific AQPs is silenced or upregulated (Kaldenhoff et al. 2008).

Local water availability and its distribution in bud and shoot bearer

At the tree scale, Vilagrosa et al. (2003, 2012) found on Mediterranean shrubs that higher resistance to cavitation was not necessarily correlated with higher survival behaviour under field conditions. This result is in line with our observations since all the trees were able to re-sprout after >4 weeks of water shortage, even if the xylem became completely embolized. Hence we can conclude that a temporary total embolism of the xylem does not necessarily imply immediate death of the plant. Moreover, we suggest that cavitation events in the xylem can be a mechanism that would allow availability of free water for vital tissues like buds. This mechanism can contribute to the maintenance of the bud moisture content that is necessary to ensure a minimal metabolic activity during water stress events.

Comparison between microcalorimetry and MRI measurements showed similar patterns (Figures 1c and d): both are quite sensitive and show a slight increase between Day 28 and Day 32. Moreover, the proton density and the relaxation time T2 followed the same pattern (Table 1). This demonstrates that the free water is extracted first when water is removed (Bottemley et al. 1986). It is commonly accepted that the lower water content leads to higher proportion of bound water and a decrease in mean T2.

Since the cambium contains meristematic cells we can assume that it is a key compartment that must be protected from drying to ensure the tree survival. The cambium proton density is high and shows high T2 values. This observation suggests that the water contained in this area is movable and could be used locally or by the surrounding connected tissues. However, at the end of the experiment, the cambium was still partly hydrated although the bud got completely dehydrated and died. Nevertheless, the T2 values became low, this being a typical feature of bound water that is not movable or usable. In the same time, none of the study trees have been able to recover after re-watering. We conclude that the hydration of the secondary meristem is not a sufficient condition for tree survival.

Conclusion

This study presents a quantitative evaluation of *P. nigra* tree bud survival during a severe water stress event. We followed the progress of bud behaviour and that of close surrounding tissues by combining 3D imaging, molecular tools and physiological measurements. The results reveal that the bud is a very resistant organ able to withstand several weeks of prolonged water deprivation. We find a close correlation between bud

respiration rate, water content and proton density. Bud moisture content can be taken as a bud mortality tipping point even in leafless trees. Moreover, 3D RMN imaging shows that this bud resistance to water stress could be due to hydraulic connections with highly hydrated tissues located in the stem and around the pith.

Overall, this study provides the first insights into a possible water distribution between connected tissues within water-stressed plants, hydraulic trade-offs between the meristematic zone integrity and the hydration of the bud and its surrounding tissues. It also reveals the implication of molecular actors during water stress events. Combining 3D NMR imaging, molecular tools and physiological measurements opens up new perspectives to understand the roles played by each tissue and their interactions in plant drought resistance.

Supplementary data

Supplementary data for this article are available at *Tree Physiology* Online.

Acknowledgments

We thank N. Lajoinie, C. Bodet, C. Serre, P. Conchon, P. Chaleil and A. Faure for plant care and handling, and for their field assistance. We also thank the anonymous reviewers for evaluating the manuscript and for their comments, and N. Boirie, J. Garcia-Sanches and ATT for language editing.

Conflict of interest

None declared.

Funding

This research was fully funded by the Institut National de la Recherche Agronomique (INRA), France.

References

- Alder NN, Sperry JS, Pockman WT (1996) Root and stem xylem embolism, stomatal conductance and leaf turgor in *Acer grandidentatum* populations along a soil moisture gradient. *Oecologia* 105:293–301.
- Alexandersson E, Fraysse L, Sjövall-Larsen S, Gustavsson S, Fellert M, Karlsson M, Johanson U, P (2005) Whole gene family expression and drought stress regulation of aquaporins. *Plant Mol Biol Reporter* 59:469–484.
- Aloni R (1987) Differentiation of vascular tissues. *Annu Rev Plant Physiol* 38:179–204.
- Aloni R, Langhans M, Aloni E, Dreieicher E, Ullrich CI (2005) Root-synthesized cytokinin in *Arabidopsis* is distributed in the shoot by the transpiration stream. *J Exp Bot* 56:1535–1544.

- Ameglio T, Archer P, Cohen M, Valancogne C, Daudet FA, Dayau S, Cruziat P (1999) Significance and limits in the use of predawn leaf water potential for tree irrigation. *Plant Soil* 207:155–167.
- Amthor JS (1994) Plant respiratory responses to the environment and their effects on the carbon balance. In: Wilkinson RE (ed.) *Plant–environment interactions*. Marcel Dekker, New York, pp 501–554.
- Atkin OK, Macherel D (2009) The crucial role of plant mitochondria in orchestrating drought tolerance. *Ann Bot* 103:581–597.
- Bartolini S, Giorgelli F (1994) Observations on development of vascular connections in two apricot cultivars. *Adv Hortic Sci* 8:97–100.
- Bennett T, Sieberer T, Willett B, Booker J, Luschig C, Leyser O (2006) The *Arabidopsis* MAX pathway controls shoot branching by regulating auxin transport. *Curr Biol* 16:553–563.
- Berleth T, Mattsson J, Hardtke CS (2000) Vascular continuity and auxin signals. *Trends Plant Sci* 5:387–393.
- Bienert GP, Bienert MD, Jahn TP, Boutry M, Chaumont F (2011) Solanaceae XIPs are plasma membrane aquaporins that facilitate the transport of many uncharged substrates. *Plant J* 66:306–317.
- Blum A (2009) Effective use of water (EUW) and not water-use efficiency (WUE) is the target of crop yield improvement under drought stress. *Field Crops Res* 112:119–123.
- Bottemley PA, Rogers HH, Foster TH (1986) NMR imaging shows water distribution and transport in plant-root systems in situ. *Proc Natl Acad Sci USA* 83:87–89.
- Braatne JH, Hinckley TM, Stettler RF (1992) Influence of soil water on the physiological and morphological components of plant water balance in *Populus trichocarpa*, *Populus deltoides* and their F1 hybrids. *Tree Physiol* 11:325–339.
- Bradshaw HD, Ceulemans R, Davis J, Stettler R (2000) Emerging model systems in plant biology: poplar (*Populus*) as a model forest tree. *J Plant Growth Regul* 19:306–313.
- Bréda N, Huc R, Granier A, Dreyer E (2006) Temperate forest trees and stands under severe drought: a review of ecophysiological responses, adaptation processes and long-term consequences. *Ann For Sci* 63:625–644.
- Brodribb TJ, Cochard H (2009) Hydraulic failure defines the recovery and point of death in water-stressed conifers. *Plant Physiol* 149:575–584.
- Brodribb TJ, Feild TS (2000) Stem hydraulic supply is linked to leaf photosynthetic capacity: evidence from New Caledonian and Tasmanian rainforests. *Plant Cell Environ* 23:1381–1388.
- Brodribb TJ, Holbrook NM, Edwards EJ, Gutierrez MV (2003) Relations between stomatal closure, leaf turgor and xylem vulnerability in eight tropical dry forest trees. *Plant Cell Environ* 26:443–450.
- Chang S, Puryear J, Cairney J (1993) A simple and efficient method for isolating RNA from pine trees. *Plant Mol Biol Rep* 11:113–116.
- Cochard H, Coste S, Chanson B, Guehl JM, Nicolini E (2005) Hydraulic architecture correlates with bud organogenesis and primary shoot growth in beech (*Fagus sylvatica*). *Tree Physiol* 25:1545–1552.
- Cook NC, Jacobs G (2000) Progression of apple (*Malus x domestica* Borkh.) bud dormancy in two mild winter climates. *J Hortic Sci Biotechnol* 75:233–236.
- Criddle RS, Fontana AJ, Rank DR, Paige D, Hansen LD, Breidenbach RW (1991) Simultaneous measurement of metabolic heat rate, CO₂ production and O₂ consumption by microcalorimetry. *Anal Biochem* 194:413–417.
- Danielson JAH, Johanson U (2008) Unexpected complexity of the aquaporin gene family in the moss *Physcomitrella patens*. *BMC Plant Biol* 8:45–60.
- de Fay E, Vacher V, Humbert F (2000) Water-related phenomena in winter buds and twigs of *Picea abies* L. (Karst.) until bud-burst: a biological, histological and NMR study. *Ann Bot* 86:1097–1107.
- Domec JC, Scholz FG, Bucci SJ, Meinzer FC, Goldstein G, Villalobos-Vega R (2006) Diurnal and seasonal variation in root xylem embolism in neotropical savanna woody species: impact on stomatal control of plant water status. *Plant Cell Environ* 29:26–35.
- Egea J, Burgos L (1994) CLIMA and doublekerneled fruits in almond. *Acta Hortic* 373:219–224.
- Escobedo J, Crabbe J (1989) Correlative control of early stages of flower bud initiation in 'bourse' shoots of apple (*Malus x domestica* Borkh., cv. Golden Delicious). *Ann Sci For* 46:44s–46s.
- Fetter K, Van Wilder V, Moshelion M, Chaumont F (2004) Interaction between plasma membrane aquaporins modulate their water channel activity. *Plant Cell* 16:215–228.
- Flexas J, Bota J, Loreto F, Cornic G, Sharkey TD (2004) Diffusive and metabolic limitations to photosynthesis under drought and salinity in C₃ plants. *Plant Biol* 6:269–279.
- Flexas J, Galmes J, Ribas-Carbo M, Medrano H (2005) The effects of drought in plant respiration. In: Lambers H, Ribas-Carbo M (eds) *Plant respiration: from cell to ecosystem*. Kluwer Academic Publishers, Dordrecht, pp 85–94.
- Gardea AA, Moreno YM, Azarenko AN, Lombard PB, Daley LS, Criddle RS (1994) Changes in the metabolic properties of grape buds during development. *J Am Soc Hortic Sci* 119:756–760.
- Gibon Y, Pyl ET, Sulpice R, Lunn JE, Höhne M, Günther M, Stitt M (2009) Adjustment of growth, starch turnover, protein content and central metabolism to a decrease of the carbon supply when *Arabidopsis* is grown in very short photoperiods. *Plant Cell Environ* 32:859–874.
- Grace J (1993) Consequences of xylem cavitation for plant water deficits. In: Smith JAC, Griffiths H (eds) *Water deficits. Plant responses from cell to community*. Bios Scientific Publishers Limited, Oxford, UK, pp 109–128.
- Grbic V, Bleecker AB (2000) Axillary meristem development in *Arabidopsis thaliana*. *Plant J* 21:215–223.
- Hacke UG (2000) Drought experience and cavitation resistance in six shrubs from the Great Basin, Utah. *Basic Appl Ecol* 1:31–41.
- Hansen LD, Criddle RS (1990) Determination of phase changes and metabolic rates in plant tissues as a function of temperature by heat conduction DSC. *Thermochim Acta* 160:173–192.
- Hansen LD, Lewis EA, Eatough DJ, Fowler DP, Criddle RS (1989) Prediction of long-term growth rates of larch clones by calorimetric measurement of metabolic heat rates. *Can J For Res* 19:609–611.
- Hansen LD, Hopkin MS, Criddle RS (1997) Plant calorimetry: a window to plant physiology and ecology. *Thermochim Acta* 300:183–197.
- Hansen LD, Macfarlane C, McKinnon N, Smith BN, Criddle RS (2004) Use of calorespirometric ratios, heat per CO₂ and heat per O₂, to quantify metabolic paths and energetics of growing cells. *Thermochim Acta* 422:55–61.
- Herter FG, Finardi NL, Mauget JC (1988) Dormancy development in apple trees cvs Gala, Golden and Fuji in Pelotas, RS. *Acta Hortic* 232:109–115.
- Hinckley TM, Braatne JH, Ceulemans R, Clum P, Dunlap J, Newman D, Smit B, Scarascia-Mugnozza G, van Volkenburgh E (1992) Growth dynamics and canopy structure of fast growing trees. In: Mitchell PK, Sennerby-Forsee L, Hinckley TM (eds) *Ecophysiology of short rotation forest crop*. Elsevier, London, pp 1–34.
- Holbrook NM, Zwieniecki MA (2005) *Vascular transport in plants. Physiological ecology*, 1st edn. Elsevier/Academic, Oxford, 564 pp.
- Huang CY, Boyer JS, Vanderhoef LN (1975) Acetylene reduction (nitrogen fixation) and metabolic activities of soybean having various leaf and nodule water potentials. *Plant Physiol* 56:222–227.
- IPCC (2007) *Climate change 2007. The physical science basis: contribution of working group I to the fourth assessment report of the Intergovernmental Panel on Climate Change*, 2007. Cambridge University Press, Cambridge, UK and New York, NY, USA, 996 pp.
- Kalcsits LA, Silim S, Tanino K (2009) Warm temperature accelerates short photoperiod-induced growth cessation and dormancy

- induction in hybrid poplar (*Populus* x spp.). *Trees Struct Funct* 23:971–979.
- Kaldenhoff R, Ribas-Carbo M, Flexas J, Lovisolo C, Heckwolf M, Uehlein N (2008) Aquaporins and plant water balance. *Plant Cell Environ* 31:658–666.
- Kang J, Tang J, Donnelly P, Dengler N (2003) Primary vascular pattern and expression of ATHB-8 in shoots of *Arabidopsis*. *New Phytol* 158:443–454.
- Kozlowski TT, Pallardy SG (1997) *Physiology of woody plants*, 2nd edn. Academic Press, San Diego, 411 pp.
- Lavender DP (1991) Measuring phenology and dormancy. In: Lassoie JP, Hinckley TM (eds) *Techniques and approaches in forest tree eco-physiology*. CRC Press, Boca Raton, pp 403–422.
- Llamas J, Carvajal-Millan E, Rascon-Chu A, Orozco JA, Gardea AA (2000) Microcalorimetry: an accurate tool for expedite determinations of plant tissue metabolism. In: Perez-Gonzalez S, Dennis F, Mondragon C, Byrne C (eds) *6th International Symposium on Temperate Fruit Growing in the Tropics and Subtropics*. Acta Horticulturae, International Society Horticultural Science, PO Box 500, 3001 Leuven 1, Belgium Queretaro Mexico, pp 79–85.
- Lopez D, Bronner G, Brunel N, et al. (2012) Insights into *Populus* XIP aquaporins: evolutionary expansion, protein functionality, and environmental regulation. *J Exp Bot* 63:2217–2230.
- Maherali H, Pockman WT, Jackson RB (2004) Adaptive variation in the vulnerability of woody plants to xylem cavitation. *Ecology* 85: 2184–2199.
- Marks PL (1975) On the relation between extension growth and successional status of deciduous trees of the Northeastern United States. *Bull Torrey Bot Club* 102:172–177.
- Matheson S, Ellingson DJ, McCarlie VW, Smith BN, Criddle RS, Rodier L, Hansen LD (2004) Determination of growth and maintenance coefficients by calorimetry. *Funct Plant Biol* 31:929–939.
- Maurel C, Verdoucq L, Luu D-T, Santoni V (2008) Plant aquaporins: membrane channels with multiple integrated functions. *Annu Rev Plant Biol* 59:595–624.
- Maurel C, Santoni V, Luu D-T, Wudick MM, Verdoucq L (2009) The cellular dynamics of plant aquaporin expression and functions. *Curr Opin Plant Biol* 12:690–698.
- McDowell NG (2011) Mechanisms linking drought, hydraulics, carbon metabolism, and vegetation mortality. *Plant Physiol* 155:1051–1059.
- Monserat-Martí G, Camarero JJ, Palacio S, Pérez-Rontomé C, Milla R, Albuixech J, Maestro M (2009) Summer-drought constrains the phenology and growth of two co-existing Mediterranean oaks with contrasting leaf habit: implications for their persistence and reproduction. *Trees Struct Funct* 23:787–799.
- Munné-Bosch S, Alegre L (2004) Die and let live: leaf senescence contributes to plant survival under drought stress. *Funct Plant Biol* 31:203–216.
- Ongaro V, Bainbridge K, Williamson L, Leyser O (2008) Interactions between axillary branches of *Arabidopsis*. *Mol Plant* 1:388–400.
- Pfaffl MW (2001) A new mathematical model for relative quantification in real-time RT-PCR. *Nucleic Acids Res* 29:2003–2007.
- R Development Core Team (2011) *R: a language and environment for statistical computing*. The R Foundation for Statistical Computing. Vienna, Austria.
- Rasband WS (1997–2009) *ImageJ*. US National Institutes of Health, Bethesda, MD.
- Rinne P, Tuominen H, Junttila O (1994) Seasonal changes in bud dormancy in relation to bud morphology, water and starch content, and abscisic acid concentration in adult trees of *Betula pubescens*. *Tree Physiol* 14:549–561.
- Rood S, Patino S, Coombs K, Tyree M (2000) Branch sacrifice: cavitation-associated drought adaptation of riparian cottonwoods. *Trees Struct Funct* 14:248–257.
- Rozen S, Skaletsky H (2000) Primer3 on the WWW for general users and for biologist programmers. *Methods Mol Biol* 132:365–386.
- Scholander PF, Hammel HT, Bradstreet ED, Hemmingsen EA (1965) Sap pressure in vascular plants. *Science* 148:339–346.
- Schulze ED (1993) Soil water deficits and atmospheric humidity as environmental signals. In: Smith JAC, Griffiths H (eds) *Water deficits: plant responses from cell to community*. BIOS Scientific Publishers Limited, Oxford, UK, pp 129–145.
- Secchi F, Zwieniecki MA (2010) Patterns of PIP gene expression in *Populus trichocarpa* during recovery from xylem embolism suggest a major role for the PIP1 aquaporin subfamily as moderators of refilling process. *Plant Cell Environ* 33:1285–1297.
- Sperry JS, Saliendra NZ, Pockman WT, Cochard H, Cruziat P (1996) New evidence for large negative xylem pressures and their measurement by the pressure chamber method. *Plant Cell Environ* 19:427–436.
- Sperry JS, Adler FR, Campbell GS, Comstock JP (1998) Limitation of plant water use by rhizosphere and xylem conductance: results from a model. *Plant Cell Environ* 21:347–359.
- Taiz L, Zeiger E (1998) *Plant physiology*, 2nd edn. Sinauer Associates Inc., MA, 792 pp.
- Thapa G, Dey M, Sahoo L, Panda SK (2011) An insight into the drought stress induced alterations in plants. *Biol Plant* 55:603–613.
- Trejo-Martínez MA, Orozco JA, Almaguer-Vargas G, Carvajal-Millan E, Gardea AA (2009) Metabolic activity of low chilling grapevine buds forced to break. *Thermochim Acta* 481:28–31.
- Turner NC (1988) Measurement of plant water status by the pressure chamber technique. *Irrig Res* 9:289–308.
- Tyree MT, Sperry JS (1988) Do woody plants operate near the point of catastrophic xylem dysfunction caused by dynamic water stress? *Plant Physiol* 88:574–580.
- Tyree MT, Zimmermann MH (2002) *Xylem structure and the ascent of sap*. Springer series in wood science, 2nd edn. Springer, Berlin, 283 pp.
- van der Schoot C, Rinne PLH. 1999. Networks for shoot design. *Trends Plant Sci* 4:31–37.
- Vilagrosa A, Cortina J, Gil-Pelegrin E, Bellot J (2003) Suitability of drought-preconditioning techniques in Mediterranean climate. *Restor Ecol* 11:208–216.
- Vilagrosa A, Chirino E, Peguero JJ, Barigah TS, Cochard H, Gil-Pelegrin E (2012) Xylem cavitation and embolism in plants living in water-limited ecosystems. In: Aroca R (ed.) *Plant responses to drought stress*. Springer, Berlin, pp 63–109.
- Wang X, Li Y, Ji W, Bai X, Chen LJ, Zhu YM (2011) A novel glycine soja tonoplast intrinsic protein gene responds to abiotic stress and depresses salt and dehydration tolerance in transgenic *Arabidopsis thaliana*. *J Plant Physiol* 168:1241–1248.
- Wardlaw IF (1990) The control of carbon partitioning in plants. *New Phytol* 116:341–381.
- Ye ZH (2002) Vascular tissue differentiation and pattern formation in plants. *Annu Rev Plant Biol* 53:183–202.